# Range-Doppler Algorithm with Extended Number of Looks

Oleksandr O. Bezvesilniy, Ievgen M. Gorovyi, Volodymyr V. Vynogradov, Dmytro M. Vavriv
Department of Microwave Electronics, Institute of Radio Astronomy of NAS of Ukraine
4 Chervonopraporna Str., Kharkov 61002, Ukraine
vavriv@rian.kharkov.ua, gorovoy@rian.kharkov.ua

*Abstract*— **Instabilities of the antenna beam orientation lead to radiometric errors in SAR images. This is one of the most difficult problems for the application of the range-Doppler algorithm, which implies a straight-line flight with a constant orientation. In the paper, we propose a radiometric correction approach for compensation of such instabilities.**

***Keywords— synthetic aperture radar; radiometric correction; SAR looks; motion compensation.***

## I. INTRODUCTION

Synthetic aperture radar (SAR) is an effective instrument for obtaining high-resolution maps of earth surfaces. The range-Doppler algorithm (RDA) [1] is one of the most popular SAR processing algorithms. Its main advantages are related with its high computational efficiency and simplicity of implementation.

The RDA performs processing of data blocks in the azimuth frequency domain assuming constant flight parameters, namely: the flight altitude and velocity as well as the antenna beam orientation. Trajectory instabilities are accounted by using some motion compensation procedures (MoCo) [2]. The application of such procedures requires an accurate measurement of the real trajectory. A more serious problem is related with accounting of variations of the antenna beam orientation. Moreover, the application of the conventional MoCo algorithms complicates the solution of this problem. Significant orientation instabilities lead to strong radiometric distortions in SAR images [3, 4]. Antenna stabilization is the most radical solution of the problem, but this is a rather expensive approach that typically can be used in the case of heavy SAR platforms.

In this paper, we propose a novel solution to the compensation of the antenna orientation instabilities on SAR images. This solution involves SAR processing with an extended number of SAR looks. By extending the processed Doppler bandwidth and, consequently, the number of SAR looks, we compensate variations of the antenna beam orientation, as shown in Fig. 1. In the figure, solid lines show a real antenna beam at two different orientations, and thin lines indicate synthetic beams of all SAR looks. Despite of the instabilities, some of the SAR looks are fit into the real antenna beam. We will show in the next sections how to combine the extended number of SAR looks to obtain SAR images without radiometric errors.

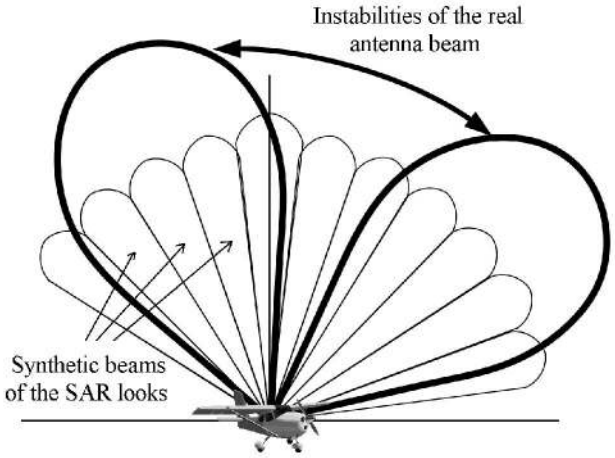


Figure 1. Processing with an extended number of looks.

## II. RDA AND MOCO

### A. Range-Doppler Algorithm

The processing steps of the RDA [1] are as follows. First, the range-compressed data are transformed into the range-Doppler frequency domain by applying the fast Fourier transform (FFT) in the azimuth. Second, the range migration correction is performed in the frequency domain. Then, the phase compensation for the azimuth compression is applied. Finally, the SAR image is formed by using the inverse FFT in the azimuth.

Multi-look (ML) processing is typically used for the suppression of speckle noise in SAR images. In the RDA, the ML processing is performed in the frequency domain by dividing the Doppler band of the backscattered radar signal into segments. By applying a separate inverse FFT to each segment of the Doppler spectrum one can build several SAR images called SAR looks. The SAR looks are summed up incoherently to reduce speckle noise.

The number of the SAR looks is usually determined as

$$NL = \mathrm{int}\left\{\frac{BW_{Ant}}{BW(\rho_X)/2}\right\} - 1 . \quad (1)$$

978-1-4244-9644-0/11/$26.00 ©2011 IEEE

Here

$$BW_{Ant} \approx \frac{2}{\lambda} V_X \theta_{Ant} \qquad (2)$$

is the Doppler bandwidth of the antenna beam, where $\lambda$ is the radar wavelength, $V_X$ is the aircraft velocity, and $\theta_{Ant}$ is the real antenna beam width. The Doppler bandwidth $BW(\rho_X)$ and the azimuth resolution $\rho_X$ are related as

$$BW(\rho_X) = K_w \frac{V_X}{\rho_X}, \qquad (3)$$

$K_w$ is the coefficient due to a weighting window applied for a side-lobe control of the synthetic aperture pattern.

### *B. Motion Compensation*

The RDA processes blocks of raw data called data frames. The algorithm assumes that the aircraft goes along a straight trajectory with a constant orientation during the time of the data frame accumulation. But in general, flight trajectory is curved, and it leads to a degradation of the SAR image quality. The MoCo procedures [2] have been proposed for accounting of flight instabilities. Such procedures perform a correction of phase and range migration errors in the SAR raw data.

The geometry of the motion compensation problem is illustrated in Fig. 2. The point $A(0, 0, H_0)$ indicates a required aircraft position on the reference flight line, and the point $A_E(\Delta x, \Delta y, H)$ corresponds to the actual position on the real trajectory. The slant range error for the synthetic beam directed to the point $P(x_P, y_P, 0)$ can be written as

$$\Delta R_E(x_P, y_P) = R_E(x_P, y_P) - R(x_P, y_P), \qquad (4)$$

where

$$R(x_P, y_P) = \sqrt{x_P^2 + y_P^2 + H_0^2},$$
$$R_E(x_P, y_P) = \sqrt{(\Delta x - x_P)^2 + (\Delta y - y_P)^2 + H^2}.$$

These relations describe both the range migration errors and the corresponding phase errors

$$\varphi_E(x_P, y_P) = -\frac{4\pi}{\lambda} \Delta R_E(x_P, y_P) \qquad (5)$$

caused by deviations of the trajectory.

The MoCo procedure performs a correction of the range migration errors (4) and phase errors (5) so that the compensated raw data seem to be collected from the reference straight-line trajectory.

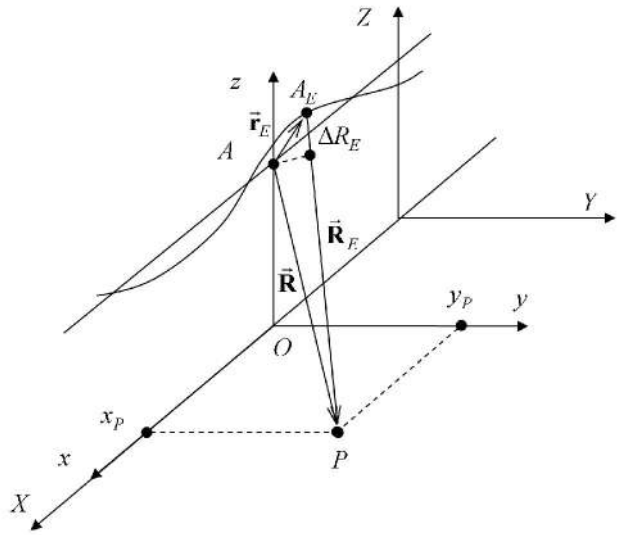


Figure 2. Geometry of the motion compensation problem.

The application of the RDA to the corrected data results in well-focused SAR images. However the MoCo procedure does not compensate the instabilities of the real antenna beam orientation, and radiometric errors are still presented.

## III. Doppler Centroid Variations Caused by MoCo

The antenna beam orientation is described by the angles $\alpha$ and $\beta$ as shown in Fig. 3. The coordinate system $(x, y, z)$ is a local coordinate system. Its *x*-axis is always directed along the horizontal component of the aircraft velocity so that $v_y = 0$.

The central Doppler frequency (Doppler centroid) for this case is

$$F_{DC} = \frac{2}{\lambda} \frac{x_R v_x - H v_z}{R}, \qquad (6)$$

where $x_R = H \tan\alpha \cos\beta + \sin\beta \sqrt{R^2 - H^2 - (H \tan\alpha)^2}$. The Doppler centroid $F_{DC}$ (6) depends on the antenna orientation angles $\alpha$ and $\beta$, the flight height $H$, and the slant range $R$.

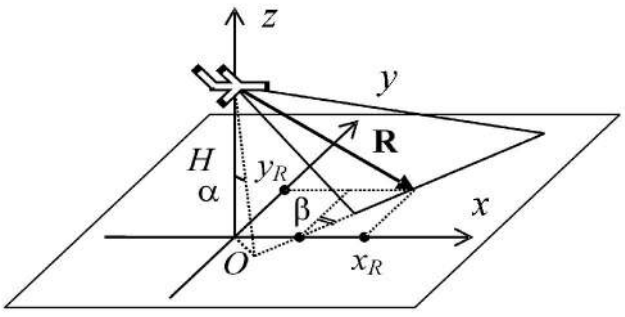


Figure 3. The antenna beam orientation angles.

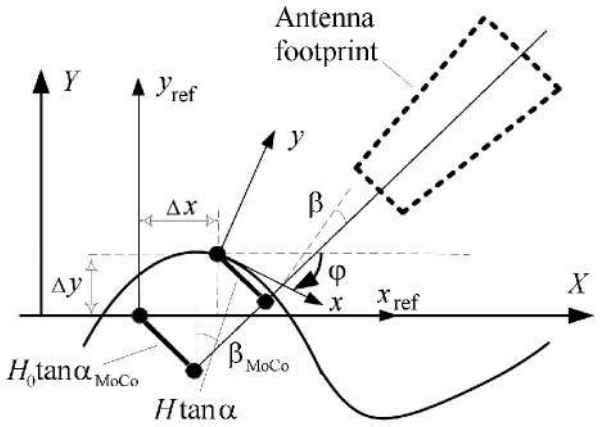


Figure 4. Flight geometry on the ground plane.

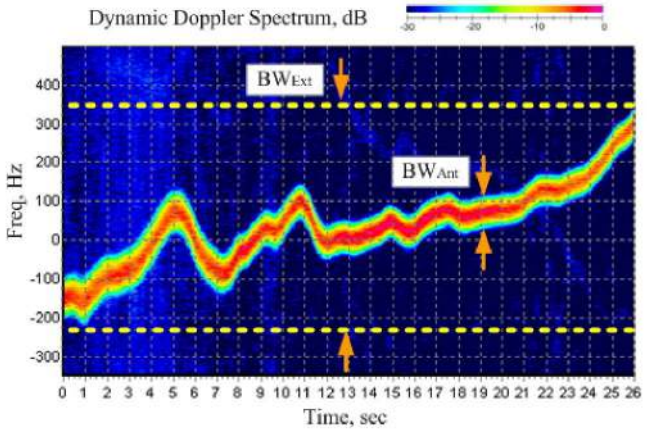


Figure 5. The dynamic Doppler spectrum of the radar data after MoCo.

After applying MoCo, the corrected raw data demonstrate range migration and phase behavior as if the data were collected from the reference straight trajectory. However, the illumination of the scene by the real antenna has not changed. In order to describe the location of the antenna footprint on the ground with respect to the position of the aircraft on the reference trajectory, we should introduce new orientation angles $\alpha_{MoCo}$ and $\beta_{MoCo}$. The geometry is illustrated in Fig. 4. One can derive the following relations for these angles:

$$\beta_{MoCo} = \beta - \varphi\,, \tag{7a}$$

$$H_0 \tan\alpha_{MoCo} = H\tan\alpha + \Delta x\cos\beta - \Delta y\sin\beta\,. \tag{7b}$$

The angle $\varphi$ describes the orientation of the horizontal component of the velocity vector $\vec{\mathbf{V}}_{XY}$ with respect to the reference line. In other words, it is the angle between the reference and the actual local coordinate systems. $H_0$ is the reference flight altitude. The actual position of the aircraft with respect to its reference position is described by shifts $\Delta x, \Delta y$.

The angles $\alpha_{MoCo}$ and $\beta_{MoCo}$ (7) as well as the Doppler centroid values (6) after MoCo are different from the angles $\alpha$, $\beta$, and the corresponding Doppler centroid values before MoCo. The changes are caused independently 1) by trajectory deviations described by the shifts $\Delta x$, $\Delta y$, and the flight altitude $H$, and 2) by the variations of the flight direction represented by the angle $\varphi$. Even if the antenna orientation is constant with respect to the actual local coordinate system ($\alpha$, $\beta$ are constant), the orientation of the antenna beam will demonstrate variations with respect to the reference flight line ($\alpha_{MoCo}$ and $\beta_{MoCo}$ change). It means that the raw data with the constant Doppler centroid could demonstrate Doppler centroid variations after applying a MoCo procedure. This effect becomes more significant in the case of a notably curved trajectory.

For the correct processing of the raw SAR data, an extended Doppler bandwidth should be selected for each data frame as follows:

$$BW_{Ext} = BW_{Ant} + \Delta F_{DC}\,, \tag{8}$$

where $\Delta F_{DC}$ is the Doppler centroid variations due to instabilities of the trajectory and antenna orientation.

An example of the dynamic Doppler spectrum calculated from raw data after applying MoCo is shown in Fig. 5. These data were obtained with a Ku-band airborne SAR [5] developed at the Institute of Radio Astronomy. The real antenna beam width is $1°$. In this case, the Doppler bandwidth of the antenna beam $BW_{Ant}$ (2) is about 100 Hz. In Fig. 5, we see significant variations of the Doppler centroid values so that the extended Doppler bandwidth is about 550 Hz.

In order to correct radiometric errors, we should increase the number of SAR looks to cover the extended Doppler bandwidth (8). The extended number of SAR looks is

$$NL_{Ext} = \mathrm{int}\left\{\frac{BW_{Ext}}{BW(\rho_X)/2}\right\} - 1\,. \tag{9}$$

Our next task is to combine all these looks into a ML SAR image correcting radiometric errors.

## IV. Radiometric Correction

Let us denote the error-free SAR image to be reconstructed as $I_0(x, y)$. The obtained SAR looks, $I(l; x, y)$, $l$ is the look index, are corrupted by speckle noise $N(l; x, y)$ and distorted by the radiometric errors $0 < R(l; x, y) \le 1$. Thus, the SAR look image can be written as

$$I(l; x, y) = I_0(x, y) \cdot N(l; x, y) \cdot R(l; x, y) \tag{10}$$

To estimate the brightness of the SAR image corrupted by radiometric errors, we can apply a two-dimensional low-pass filter. This filter suppresses speckle noise but preserves variations of the illumination. The smoothed image can be written approximately as

$$I_{LF}(l; x, y) \approx I_{0LF}(x, y) R_{LF}(l; x, y). \quad (11)$$

Here $I_{0LF}(x, y)$ is the filtered component of the SAR image, and $R_{LF}(l; x, y)$ is the smoothed radiometric error function. We shall assume that the high-frequency component of the radiometric errors is small so that $R_{LF}(l; x, y) \approx R(l; x, y)$.

Each part of the scene is always presented in several SAR look images. From all of the extended SAR looks we should compose only several "best" SAR looks, selecting the best-illuminated parts of the images, by comparing the brightness of their low-frequency versions (11) pixel-by-pixel. The number of the composed looks $NL_{Best}$ is approximately equal or slightly less than the number of looks $NL$ (1), which fit into the antenna beam. The composed looks could be sorted in ascending order according to their brightness.

The idea of the radiometric correction is based on the fact that at least one of the extended looks is pointed very close to the center of the real antenna beam. This look has the maximum power and does not suffer of radiometric errors. For this look $R(x, y) \approx 1$, and, according to (11), we can use it as a reference to estimate the error-free low-frequency component of SAR image: $I_{0LF}^{Est}(x, y) \approx I_{Best\,LF}(x, y)$. Now we can find the radiometric error functions from (11) as

$$R_{Est}(l; x, y) \approx \frac{I_{LF}(l; x, y)}{I_{0LF}^{Est}(x, y)}. \quad (12)$$

Applying the above radiometric correction to all SAR looks, we can build the multi-look SAR image as

$$I_{NL_{Best}}(x, y) = \frac{1}{NL_{Best}} \sum_{l=1}^{NL_{Best}} I_{Best}(l; x, y) \frac{I_{0LF}^{Est}(x, y)}{I_{Best\,LF}(l; x, y)}. \quad (13)$$

## V. Results

The SAR image shown in Fig. 6a is built of 9 central looks without radiometric correction. It is corrupted by radiometric errors. The SAR image in Fig. 6b was obtained by simple averaging of all 83 extended SAR looks. Brightness variations are still presented on the image. The 5-look SAR image after performing the radiometric correction is shown in Fig. 6c. We can see that the radiometric errors have been successfully eliminated.

## VI. Conclusion

The proposed approach of multi-look processing with an extended number of SAR looks allows tracking of variations of the antenna orientation in the case of strong flight instabilities. The developed radiometric correction procedure is a robust and cost-effective solution as compared to the solution based on the antenna stabilization.

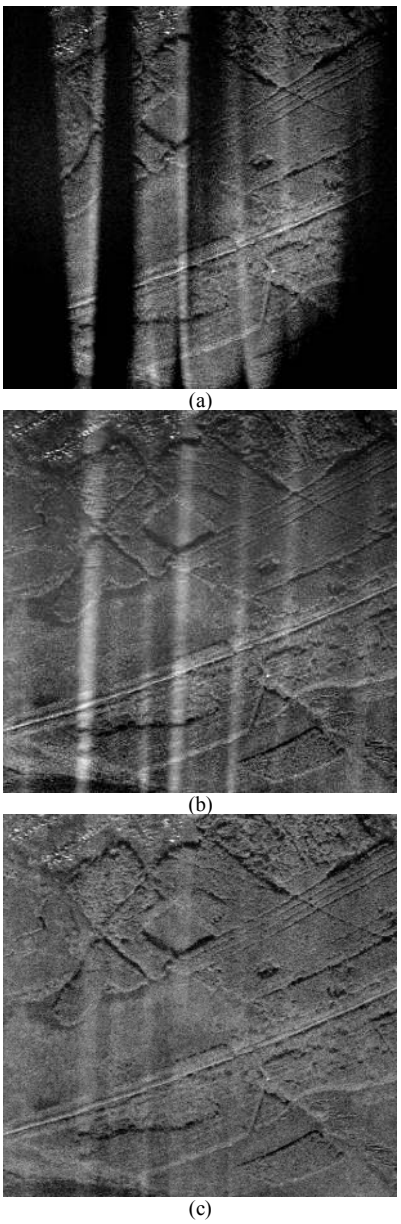

(a) (b) (c)

Figure 6. Multi-look processing with and without radiometric correction.

## References


[1] I. G. Cumming and F. H. Wong, Digital processing of synthetic aperture radar data: algorithms and implementation. Norwood, MA: Artech House, 2005, 625p.

[2] G. Franceschetti, R. Lanari. Synthetic Aperture Radar Processing. CRC Press, 1999, 328 pages.

[3] O. O. Bezvesilniy, Ie. M. Gorovyi, S. V. Sosnytskiy, V. V. Vynogradov, D. M. Vavriv, "SAR Processing Algorithm with Built-In Correction", Radio Physics and Radio Astronomy, vol. 16, no. 1, pp. 98-108, 2011.

[4] O. Frey, C. Mangard, M. Rüegg, E. Meier, "Focusing of airborne synthetic aperture radar data from highly nonlinear flight tracks", IEEE Trans. Geosci. Remote Sens., Vol. 47, No. 6, pp. 1844–1858, June 2009.

[5] D. M. Vavriv et al., "Cost-effective Ku-band airborne SAR with Doppler centroid estimation, autofocusing and indication of moving targets", Proc. 2nd European Radar Conf. EuRAD2005, pp. 21-24.